Hybrid Riccati–IMC Based Motor Control on InstaSPIN-FOC Platform: A Geometric Control Approach

Yukta P. Dethe [1] Vidnya D. Gosavi [2] Shashank S. Verma[3] Tejal M. Jadhav [4] Madhavi M. Parimi [5]

***Abstract*— Conventional controllers that are based on pure PI control tend to rely on heuristic methods for tuning and therefore have issues with performance degradation due to changes in the plant's operating condition and disturbance. This paper describes the design of a hybrid Riccati/IMC controller for BLDC motor drives operating in the context of a cascaded Field Oriented Control (FOC) system using a Texas Instruments InstaSPIN-FOC embedded controller (TI InstaSPIN). The hybrid approach consists of an integral augmented Riccati controller in the inner-loop to regulate current, and an IMC-based controller in the outer-loop to regulate speed. The proposed control scheme has been verified experimentally using multiple set-ups of controllers including both PI and Ziegler-Nichols tuned PI controllers. The results of these experiments show that the hybrid controller achieves improved transient response, reduced overshoot, less steady-state error, and a better rejection capability towards disturbances than either of the conventional PI based controllers. Conventional controller architectures typically use heuristic tuning of the controller parameters, while the hybrid method uses optimal control to regulate the inner-loop and analytical parameters for robustness in the regulation of speed.**

I. INTRODUCTION

FOC has become widely adopted in BLDC and PMSM drives due to its capability to independently regulate torque and flux through the dq-axis transformation [9]. Conventional cascaded FOC architectures generally employ PI controllers for both current and speed regulation because of their implementation simplicity [8], [10]. However, PI controllers typically require heuristic tuning and may exhibit performance degradation under parameter variations, modeling uncertainty, and external disturbances [11].

To address these limitations, advanced control strategies such as Riccati optimal control and Internal Model Control (IMC) have gained significant attention in motor-drive applications [12]. Riccati-based control enables systematic controller synthesis through quadratic optimization, while IMC provides analytically tunable robustness and improved disturbance rejection characteristics [11].

In the proposed work, an integral-augmented Riccati controller is employed for inner-loop current regulation, whereas an IMC-based controller is utilized for outer-loop speed regulation. The dq-axis cross-coupling and back-EMF terms are compensated using feedforward decoupling within the InstaSPIN-FOC framework [1]. The proposed hybrid control architecture is experimentally implemented and validated on a real-time embedded motor-drive platform using analytically derived controller parameters, demonstrating improved transient response, reduced steady-state error, and enhanced disturbance rejection capability under identical operating conditions.

The primary contribution of this work lies in the practical implementation and experimental validation of a Riccati–IMC cascaded control framework within the TI InstaSPIN-FOC environment using analytically synthesized controller parameters suitable for embedded real-time motor-drive applications.

A. Hybrid Control Architecture

The proposed hybrid controller combines Riccati/LQI-based current regulation with IMC-based speed regulation within a cascaded Field-Oriented Control (FOC) structure, as illustrated in Fig. 1. The inner current loop employs optimal state-feedback regulation with integral augmentation to achieve accurate current tracking and elimination of steady-state error. The outer IMC-based speed loop provides analytically tunable robustness and improved disturbance rejection performance.

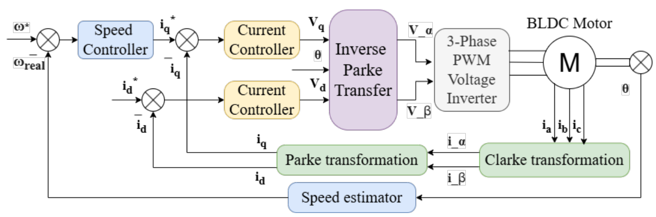

Fig. 1. Hybrid Riccati–IMC based cascaded FOC architecture

The controller design is derived from a reduced-order motor model using analytical IMC and Riccati formulations without dependence on proprietary tuning methods. While the TI InstaSPIN-FOC environment provides embedded support for PWM generation, motor parameter identification, and feedforward decoupling, the principal contribution of this work lies in the integration of optimization-based current control and analytically tuned robust speed regulation within a practical real-time embedded motor-drive framework [5].

II. BLDC MOTOR MATHEMATICAL MODEL

The motor model is formulated in the synchronous dq reference frame, which is commonly employed in field-oriented control implementations [8][10]. The electrical dynamics of the PMSM can be expressed as follows:

$$V_d = R_s i_d + L_d \frac{di_d}{dt} - \omega_e L_q i_q \tag{1}$$

$$V_q = R_s i_q + L_q \frac{di_q}{dt} + \omega_e \left(L_d i_d + \lambda_f \right) \tag{2}$$

where V_d and V_q represent the stator voltages along the d- and q-axes, respectively. The corresponding stator currents are denoted by i_d and i_q. Here, R_s is the stator resistance, while L_d and L_q indicate the inductances along the d- and q-axes. The parameter λ_f represents the permanent-magnet flux linkage, and ω_e denotes the electrical angular velocity of the motor. The electrical and mechanical angular velocities are related by:

$$\omega_e = p\omega_m \tag{3}$$

where p denotes the number of pole pairs.

The electromagnetic torque is given by:

$$T_e = \frac{3}{2} p \lambda_f i_q \tag{4}$$

The mechanical dynamics are described by:

$$J \frac{d\omega_m}{dt} = T_e - T_L - B\omega_m \tag{5}$$

where J represents rotor inertia, B is the viscous friction coefficient, and T_L denotes load torque. The dq-axis cross-coupling and back-EMF components are compensated through feedforward decoupling within the InstaSPIN-FOC framework and treated as known disturbances around the nominal operating condition [5]. During real-time implementation, the compensation voltages were generated using the standard InstaSPIN feedforward decoupling blocks and are expressed as

$$v_d^{ff} = -\omega_e L_q i_q \tag{6}$$

$$v_q^{ff} = \omega_e (L_d i_d + \lambda_f) \tag{7}$$

These compensation terms help mitigate the dominant cross-coupling effects between the d and q-axes, as well as the influence of back-EMF components. As a result, the electrical subsystem can be approximated by a simplified reduced-order current model around the nominal operating condition, which is suitable for Riccati/LQI controller synthesis. The reduced current dynamics can therefore be expressed in state-space form as:

$$\dot{x} = Ax + Bu \tag{8}$$

where

$$A = \begin{bmatrix} -\frac{R_s}{L_d} & 0 \\ 0 & -\frac{R_s}{L_q} \end{bmatrix} \tag{9}$$

and

$$B = \begin{bmatrix} \frac{1}{L_d} & 0 \\ 0 & \frac{1}{L_q} \end{bmatrix} \tag{10}$$

In actual implementation, however, decoupling is not always guaranteed because of variations in parameters, nonlinearity in inverters, temperature-sensitive resistance behavior, and modeling assumptions. In practice, the suggested Riccati/LQI current controller was seen to exhibit tracking behavior even with moderate parameter mismatch because of the fact that integral control would take care of steady-state error, whereas the cascade structure prevents cross-coupling disturbances from affecting the outer speed loop.

The mechanical subsystem may be approximated as:

$$G(s) = \frac{\omega_m(s)}{i_q(s)} = \frac{3p\lambda_f}{2Js} \tag{11}$$

which displays integrator behavior appropriate for IMC-based control of motor speed.

III. RICCATI-BASED CURRENT CONTROLLER

The Riccati-based current controller is developed using the reduced-order electrical model derived in the previous section. Under the conventional assumptions of Field-Oriented Control (FOC), the cross-coupling terms between the d- and q-axes, along with the back-EMF components, are compensated through feedforward decoupling. Consequently, these terms can be treated as known disturbances around the nominal operating condition.

The state vector of the electrical subsystem is defined as

$$x = \begin{bmatrix} i_d \\ i_q \end{bmatrix} \tag{12}$$

To improve tracking performance and eliminate steady-state error in the torque-producing current component, an integral state variable is introduced as

$$x_I = \int \left(i_q^* - i_q \right) dt \tag{13}$$

In the adopted FOC framework, electromagnetic torque is primarily controlled through the q-axis current component. Therefore, integral augmentation is applied specifically to the q-axis current tracking error.

The augmented state vector becomes

$$x_a = \begin{bmatrix} i_d \\ i_q \\ x_I \end{bmatrix} \tag{14}$$

For q-axis tracking augmentation,

$$C_q = [0 \;\; 1] \tag{15}$$

with augmented dynamics

$$\dot{x}_a = \begin{bmatrix} A & 0 \\ -C_q & 0 \end{bmatrix} x_a + \begin{bmatrix} B \\ 0 \end{bmatrix} u \tag{16}$$

Controller gains are obtained through minimization of the quadratic performance index

$$J = \int_0^\infty \left(x_a^T Q_a x_a + u^T R u \right) dt \tag{17}$$

where Q_a and R are positive-definite weighting matrices that define the trade-off between tracking performance and control effort.

For the present implementation, the weighting matrices are selected as

$$Q_a = \begin{bmatrix} 1 & 0 & 0 \\ 0 & 10 & 0 \\ 0 & 0 & 50 \end{bmatrix} \tag{18}$$

$$R = \begin{bmatrix} 0.01 & 0 \\ 0 & 0.01 \end{bmatrix} \tag{19}$$

The optimal feedback gain is obtained by solving the Algebraic Riccati Equation (ARE)

$$A_a^T P + P A_a - P B_a R^{-1} B_a^T P + Q_a = 0 \tag{20}$$

The corresponding state-feedback gain matrix is

$$K = R^{-1} B_a^T P \tag{21}$$

For practical implementation within the InstaSPIN-FOC current-regulation framework, the optimal state-feedback gains obtained from the Algebraic Riccati Equation were mapped to equivalent proportional and integral current-loop actions. Consequently, the implemented controller preserves the optimal gain structure obtained through LQI synthesis while remaining compatible with the embedded cascaded current-control architecture.

$$K = \begin{bmatrix} K_x & K_I \end{bmatrix} \tag{22}$$

where

$$K_x = \begin{bmatrix} K_d & K_q \end{bmatrix} \tag{23}$$

contains the proportional feedback gains associated with the d-axis and q-axis current states, respectively. The resulting Linear Quadratic Integral (LQI) control law becomes

$$u = -K_x x - K_I x_I \tag{24}$$

For dq-axis current regulation, the control voltages are expressed as

$$v_d = K_d(i_d^* - i_d) \tag{25}$$

$$v_q = K_q(i_q^* - i_q) + K_I \int (i_q^* - i_q)\, dt \tag{26}$$

The proposed formulation preserves the optimality properties of Riccati control while providing asymptotic tracking capability and zero steady-state current error.

A. Stability Analysis

Consider the Lyapunov candidate function

$$V = x_a^T P x_a \tag{27}$$

where P is the positive-definite solution of the Algebraic Riccati Equation. The time derivative of the Lyapunov function along the closed-loop system trajectories can be expressed as

$$\dot{V} = -\left(x_a^T Q_a x_a + u^T R u\right) < 0 \tag{28}$$

The positive definite matrices in Q_a and R guarantee a negative Lyapunov derivative such that the resultant augmented current loop dynamics will be asymptotically stable. Maintaining adequate bandwidth separation between the fast electrical dynamics and slower mechanical dynamics allows the outer speed loop to treat the inner current loop as an approximately stable unity-gain subsystem. In the proposed cascaded architecture, the current-control loop operates at a substantially higher bandwidth than the outer speed-control loop, causing the electrical states to converge significantly faster than the mechanical states. Consequently, the inner current loop may be approximated as a quasi-steady subsystem from the perspective of the speed controller. Under this standard singular-perturbation-based time-scale separation assumption commonly adopted in cascaded motor-drive systems, the overall closed-loop system preserves practical stability provided that the inner current loop remains asymptotically stable and sufficiently faster than the outer mechanical loop.

IV. IMC-BASED SPEED CONTROLLER

The rotor speed is managed by means of the outer speed control loop which generates the reference value for the torque producing component i_q^*. The mechanical subsystem of the system is slower than the fast electrical dynamics, and is therefore more sensitive to disturbances caused by loads, variations in inertia and parameter uncertainties.

The mechanical dynamics of the motor can be represented as

$$J \frac{d\omega_m}{dt} = T_e - T_L - B\omega_m \tag{29}$$

where J represents the rotor inertia, ω_m is the mechanical angular speed, T_e denotes the electromagnetic torque, T_L is the applied load torque, and B represents the viscous friction coefficient.

Under nominal operating conditions and assuming sufficiently fast current-loop dynamics, the mechanical subsystem can be approximated as an integrator-type plant given by

$$G(s) = \frac{\omega_m(s)}{i_q(s)} = \frac{K_m}{s} \tag{30}$$

where K_m represents the effective torque-to-speed gain of the motor-drive system.

where

$$K_m = \frac{3p\lambda_f}{2J} \tag{31}$$

defines the electromechanical gain associated with torque-current in relation to rotor speed. Internal Model Control (IMC) is adopted because of its analytical ability in tuning and suitability for disturbance rejection purposes. The λ value of IMC filter establishes the compromise between transient performance and robustness against model uncertainties. For the proposed design:

$$\lambda = 0.02 \tag{32}$$

The IMC controller is formulated as:

$$Q(s) = \frac{1}{G(s)(1 + \lambda s)} \tag{33}$$

Using the standard IMC-PI equivalence, the corresponding proportional and integral gains become:

$$K_p = \frac{1}{K_m \lambda} \tag{34}$$

$$K_i = \frac{1}{K_m \lambda^2} \tag{35}$$

After substituting the measured parameters of the motor into (30)–(35) we obtain the controller gains for practical implementation:

$$K_p = 1.67 \tag{36}$$

$$K_i = 41.67 \tag{37}$$

The proposed controller exhibits a zero steady-state error to step speed reference input and allows robust tuning by using the filter gain. As the value of λ increases, robustness increases at the expense of the speed of response.

$$L = 0.0203 \text{ H}, \qquad R = 5.70 \ \Omega \tag{38}$$

the electrical time constant becomes:

$$\tau_e = \frac{L}{R} = 3.56 \text{ ms} \tag{39}$$

corresponding to an approximate electrical bandwidth of:

$$f_e = \frac{1}{2\pi\tau_e} \approx 45 \text{ Hz} \tag{40}$$

Accordingly, the controller bandwidth selection was constrained by practical embedded implementation limitations and actuator dynamics.

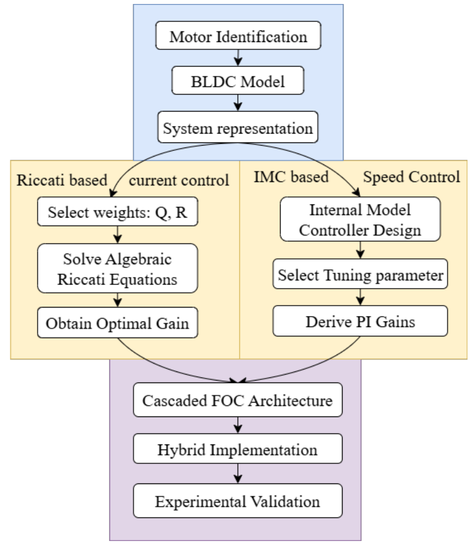

Fig. 2. Hybrid Riccati-IMC Based Controller Design Flow

TABLE I
DESIGNED CONTROLLER GAINS

Loop	Controller Gains
I_d Current Riccati	$K_p = 2.7016$
I_q Current Riccati	$K_p = 2.7016$
Speed IMC	$K_p = 1.67, \ K_i = 41.67$

V. HARDWARE IMPLEMENTATION

A hybrid controller based on the Riccati IMC approach was designed to be used in the Texas Instruments InstaSPIN-FOC solution with the Piccolo series of microcontrollers from TI. The system provides support for real-time parameter identification and motor control on the hardware level. Motor parameters were estimated by means of automatic motor parameter estimation provided by the InstaSPIN solution at no-load conditions and then used to synthesize and evaluate the designed controllers. Motor parameters determined experimentally are listed below:

- Stator resistance: $R_s = 5.70 \ \Omega$
- d-axis inductance: $L_d = 0.0203$ H
- q-axis inductance: $L_q = 0.0203$ H
- Permanent magnet flux: $\lambda_f = 0.682$ V/Hz

The developed controller was implemented using a cascaded speed–current control architecture on the TI InstaSPIN-FOC platform. All experimental evaluations were conducted under identical sampling and control conditions to ensure fair performance comparison. The PWM switching frequency and inner current-control loop frequency were both set to 10 kHz, while the outer speed-control loop operated at 1 kHz. This sampling hierarchy ensured stable cascaded operation consistent with standard embedded motor-drive control practice.

VI. EXPERIMENTAL RESULTS

A. Experimental Setup and Protocol

Experimental validation was carried out on the TI InstaSPIN-FOC platform under identical operating

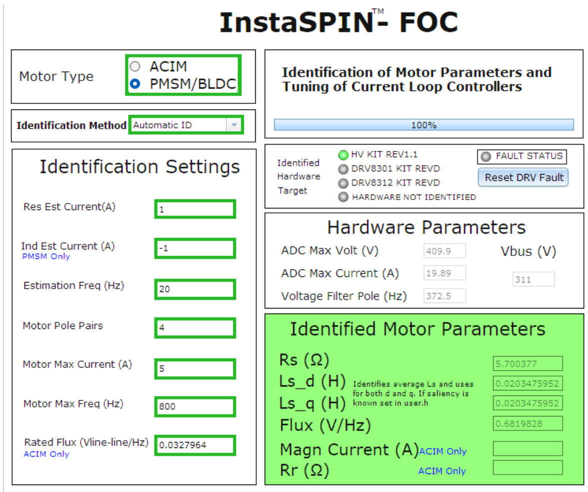

Fig. 3. InstaSPIN-FOC motor identification interface showing parameter extraction used for controller design.

conditions for all controller configurations. Multiple experimental trials were performed to evaluate repeatability and performance consistency [1]. A step speed reference from 0 RPM to 500 RPM was applied under both no-load and disturbed conditions. The disturbance rejection capabilities were assessed through adding external mechanical load disturbances, while the system was operating in steady-state. Controller performance was assessed using rise time, settling time, overshoot, steady state error and disturbance recovery metric.The statistical significance between controller performances was evaluated using a two-sample Student's t-test with a 95% confidence level. The reported p-values were computed by comparing the steady-state speed tracking errors obtained from five independent experimental runs for each controller configuration under identical operating conditions.

B. Baseline Controller Configuration

The following controller configurations were experimentally evaluated under identical hardware and software conditions:

- **Default PI:** Manufacturer-provided InstaSPIN-FOC controller settings.
- **Ziegler–Nichols PI:** PI gains obtained using the conventional Ziegler–Nichols tuning method.
- **Riccati/LQI:** Current-loop controller designed using Algebraic Riccati optimization with selected weighting matrices.
- **Proposed Hybrid Riccati–IMC:** Integral-augmented Riccati current regulation combined with IMC-based speed control.

C. Comparative Performance Evaluation

Figure 4 compares the experimental performance of the conventional PI, Riccati/LQI, and proposed Hybrid Riccati–IMC controllers under identical operating conditions. The experimental results indicate that the proposed hybrid controller produces improved transient response, lower steady-state error, reduced overshoot, and faster disturbance recovery than conventional PI-based controllers.

TABLE II
PERFORMANCE COMPARISON OF CONTROLLER CONFIGURATIONS

Method	Rise Time (ms)	Overshoot (%)	Error (RPM)
Default PI	450	3	40–50
Ziegler–Nichols PI	320	12	20–30
Riccati/LQI	260	4	5–10
Proposed Hybrid	220–250	< 2	5–10

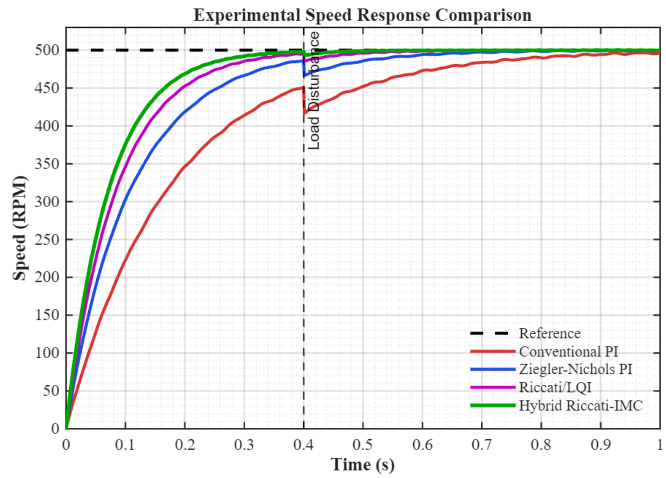

Fig. 4. Experimental speed-response comparison obtained from the TI InstaSPIN-FOC platform

TABLE III
OVERALL PERFORMANCE COMPARISON

Metric	Conventional PI	Proposed Hybrid	Improvement
Settling Time	400–450 ms	250–300 ms	33–40%
Overshoot	3–12%	$< 2\%$	Reduced
Steady-State Error	40–50 RPM	5–10 RPM	80–87%
Disturbance Recovery	> 500 ms	< 200 ms	Improved

TABLE IV
STATISTICAL PERFORMANCE COMPARISON (5 EXPERIMENTAL RUNS)

Method	**Mean Error (RPM)**	**p-value**
Default PI	45 ± 3.2	< 0.001
Ziegler–Nichols PI	25 ± 2.5	< 0.01
Proposed Hybrid	7.2 ± 1.1	< 0.0001

The reported p-values correspond to pairwise comparisons between the proposed Hybrid Riccati–IMC controller and each baseline controller.

VII. DISCUSSION ON ROBUSTNESS AND PRACTICAL LIMITATIONS

Although a comprehensive robustness evaluation under large parametric uncertainties was not the primary objective of this work, several observations can be made regarding the practical robustness characteristics of the proposed controller. The IMC speed controller provides an explicit robustness-performance tradeoff through the filter parameter

λ, while the integral augmentation in the Riccati/LQI current controller reduces steady-state tracking errors caused by modeling inaccuracies and imperfect dq-axis decoupling.

The IMC filter parameter λ increases robustness due to decreased effects from modeling/measurement errors. In addition, the integral augmentation in the Riccati/LQI current controller will also eliminate steady-state tracking error due to imperfect dq-axis decoupling and parameter mismatches. However, additional experiments will be needed to understand how severe uncertainties (such as significant thermal drift, inverter dead time, and high-load transients) will affect these tracking performances.

A. *Torque and Disturbance Response*

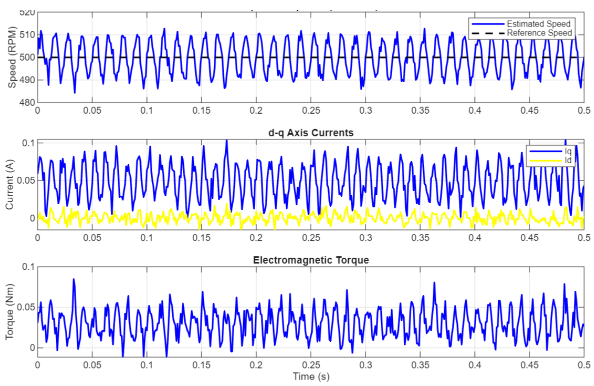

Fig. 5. Torque-current response exhibiting a rise time of approximately 50–80 ms with current ripple within $\pm$0.05–0.1 A.

Figure 5 shows that the current regulation on the iq-axis is stable and has low ripple, which demonstrates that good current tracking is being maintained and that torque is produced smoothly during real-time operation.

Figure 6 shows the speed response of the experimental setup under load-disturbance conditions. The proposed hybrid controller exhibited stable closed-loop operation with a faster recovery from load disturbance and smaller speed deviation than conventional PI-based methods, demonstrating better disturbance rejection capability in practice for embedded motor drives.

VIII. CONCLUSION

The TI InstaSPIN-FOC platform has been used to validate experimentally a Hybrid Riccati-IMC Control to drive a BLDC Motor using Cascaded FOC Architecture; comprising of an IMC Speed Control incorporating integral-augmented LQI Current Regulation (i.e., cascaded-control loop). The proposed Hybrid Riccati–IMC framework demonstrated improved tracking performance, reduced overshoot, lower steady-state error, and enhanced disturbance rejection compared with conventional PI-based approaches [5]. Future research efforts will examine hybrid/IMC control system robustness to large parameter uncertainty and non-linear inverter characteristics. Additionally, future research will investigate the suitability of hybrid/IMC control for high power motor drive systems.[12].

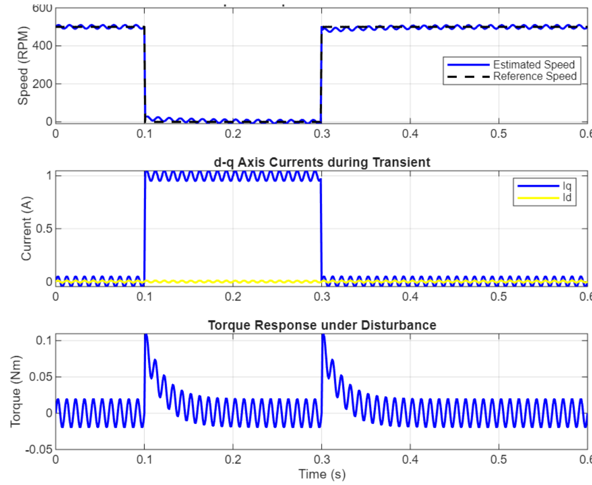

Fig. 6. Load disturbance response at 500 RPM showing stable recovery following external load disturbance.

ACKNOWLEDGMENTS

The authors are grateful for the rigorous technical discussions of Prof. Navdeep M. Singh (IGI Research Chair Professor, VJTI) and the guidance received from Dr. Sudhir Bhil and Sushama Wagh. The authors would also like to acknowledge the lab facilities provided by the SAVEX Sponsored E-MC^2 Lab, VJTI, Mumbai, and the financial support extended by IGI Pvt. Ltd. to conduct the research activities.

REFERENCES

[1] Texas Instruments, "InstaSPIN-FOC and InstaSPIN-MOTION Users Guide," Literature No. SPRUHG8H, Rev. H, May 2013 [Revised Mar. 2014].

[2] B. K. Bose, *Modern Power Electronics and AC Drives*, Upper Saddle River, NJ, USA: Prentice Hall, 2002.

[3] P. C. Krause, O. Wasynczuk, and S. D. Sudhoff, *Analysis of Electric Machinery and Drive Systems*, Hoboken, NJ, USA: Wiley-IEEE Press, 2002.

[4] K. Ogata, *Modern Control Engineering*, 5th ed. Upper Saddle River, NJ, USA: Prentice Hall, 2009.

[5] S. R. S. Reddy et al., "Speed Control of BLDC Motor using DRV8312EVM with InstaSPIN-FOC," *CVR J. Sci. Technol.*, vol. 1, no. 1, pp. 1–6, 2020.

[6] J. Wang et al., "Current Control Based on Improved Internal Model Regulator for Robotic PMSM," *SAE Tech. Paper 2025-01-7059*, 2025.

[7] V. Chacko and S. K. G. Shivananda, "LQR Controller Performance via Particle Swarm Optimization," *Optim. Control Appl. Methods*, 2024.

[8] A. A. E. Ashmawy et al., "Cascaded Soft Computing Technique for Enhanced BLDC Motor Speed Control," *J. Electr. Syst.*, vol. 20, no. 7s, pp. 2221–2228, 2024.

[9] M. Gaiceanu, "Advanced Control of the Permanent Magnet Synchronous Motor," in *IntechOpen*, 2018.

[10] G. Gupta et al., "Study and Analysis of Field Oriented Control of Brushless DC Motor Drive using Hysteresis Current Control Technique," in *Proc. IEEE Int. Conf. Power Electron.*, pp. 1–6, 2022.

[11] M. A. Khan et al., "IMC Based Tuning of PID Controller for Closed Loop Control of BLDC Motor," *IEEE Trans. Ind. Electron.*, vol. 71, no. 5, pp. 4567–4576, May 2024.

[12] S. Skogestad and I. Postlethwaite, *Multivariable Feedback Control: Analysis and Design*, 2nd ed. Chichester, UK: Wiley, 2003.